LAMINAR JET CHARACTERISTICS IN A LOUDSPEAKER INDUCED STANDING WAVE

S. A. Farhat and Y. Zhang

Mechanical Engineering Department, Faculty of Engineering, Al-Fateh University
E-mail address: salemfarhat_t@yahoo.co.uk

الملخص

تم في هذه الورقة دراسة ومناقشة تأثير الإثارة السمعية (acoustic excitation) على نمط التدفق لنفث غازي رقائقي (laminar jet) داخل إسطوانة أنبوبية. لُوحظ أن للإثارة السمعية تأثيراً قوياً على سرعة النفث وأيضاً على بنية إنسيابه (Flow structure). لقد وُجد أنه تحت تأثير الإثـــارة السمعية تزداد سرعة النفث لأكثر من سبعة أضعاف عن سرعته بدون إثارة سمعية. تم إجـــراء مقارنة تحليلية مفصلة لنمط سرعة النفث تحت تأثير الإثارة السمعية وبدون إثارة سمعية عنـــد أوضاع مختلفة فوق فتحة النفث. هناك نتائج مذهلة جديرة بالإهتمام نتيجة للإثارة السمعية حيث وجد أنه من الممكن حدوث تغير بالضغط الإستاتيكي داخل الأنبوب بأماكن مختلفـــة بالموجـــة الواقفة (Standing wave) ونتيجة لذلك حدثت زيادة بمعدل تدفق الهواء عند وضع فتحة النفـــث بمنطقة الضغط الإستاتيكي السلبي (Negative static pressure zone). عند إستبدال الهواء بوقود البروبين (C_3H_8) وتحت الإثارة السمعية لُوحظ أن لون اللهب (Diffusion flame) يتغير تمامـــاً مع إنخفاض في إرتفاعه وأن قاعدة اللهب ترتفع مبتعدةً عن فتحة النفث. هذه المشاهدات تبين أن للإثارة السمعية تأثيراً قوياً على نمط التدفق وخواص اللهب.

ABSTRACT

In this paper, the acoustic excitation effects on the flow characteristics of a laminar jet inside an air-filled cylindrical tube have been presented and discussed. It is observed that the acoustic excitation has a strong effect on the jet velocity and its flow structure. Under excitation, the velocity is observed to increase more than seven times. Comparisons and investigations of the velocity characteristics with and without excitation, at different position above the nozzle exit have been carried out in detail. An important observation is that the acoustic excitation could induce a static pressure in the cylindrical tube. As a result, an increase of air flow rate could be measured if the air nozzle is positioned in the negative static pressure zone. When under acoustic excitation and the air jet is replaced by a propane fuel jet, the laminar jet propane diffusion flame was observed to change colour, shorter in height, and lifting off at different acoustic regimes of the standing wave. These observations indicate that acoustic excitation have changed the flow and flame properties significantly. It is observed that acoustic excitation does not accelerate the flow field uniformly. The high velocity region is found to increase in value much more than in the low velocity region. To investigate the effect of acoustic excitation on flow characteristics in a confined space is of great importance.

KEYWORDS: Acoustic effects on flow structure of confined laminar jet

INTRODUCTION

In an air-filled cylindrical tube a standing wave can be generated by activating a loudspeaker at one end of the tube. The longitudinal wave travelling along the air-filled tube is reflected at the open end of the tube. Interference between the waves travelling in opposite directions gives rise to standing longitudinal waves. If the end of the tube is closed, the reflected wave is 180^o out of phase with the incident wave. At the closed end the velocity must always be zero. Therefore, a closed end is a velocity node. If the end of the tube is open, the fluid elements there are free to move. The nature of the reflection there depends on whether the tube is narrow or wide compared to the wavelength. If it is narrow, the reflected wave has nearly the same phase as the incident wave. Then the open end is almost a velocity anti-node. The location of the anti-node is usually not exactly at the opening [1].

Standing waves in a tube have been studied for many different applications, such as thermoacoustic instabilities in combustors, and the suppression of pressure oscillations, diffusion flame soot suppression [2-7]. Acoustic streaming flow allows forced convective heat transfer without any macroscopic mechanical moving parts [8]. Studies on acoustically disturbed combustion have been conducted by many researchers [9], because flame and acoustic wave coupling plays an important role in practical combustion devices. Farhat, et al [10] investigated the flame properties of a diffusion flame jet at different phases of a loudspeaker induced standing wave in a cylindrical tube. They showed that the properties of a diffusion flame jet is sensitive to the change of fuel nozzle position relative to the cylindrical tube even in the case of without acoustic excitation, which implies that the flame position inside a practical device would affect the emissions. They showed that the flame properties depend strongly on the phase of the standing wave, and the most dramatic change was observed in the rarefaction regime. In this paper the velocity characteristics of an air jet in the refraction regime is investigated in detail. Full mapping of the velocity field has been conducted. Both the acoustic pressure and the *rms* velocity fields are investigated experimentally together with a theoretical analysis of the longitudinal standing waves travelling along an air-filled tube.

EXPERIMENTAL SET UP

The experimental apparatus is shown in Figure (1). It consists of a laminar air jet inside the cylindrical tube, a signal generation and data collection system, a Constant Temperature Anemometer (CTA), a micro-manometer, a sound level meter, and a computer controlled 3D traverse system.

Air was supplied from a compressed air cylinder at initial flow rate of 150 ml/min, regulated by a control valve, and measured by a calibrated flow meter (rotameter). The air nozzle is a single copper pipe with an inner diameter of 0.5 cm. There is an orifice at the end of the pipe, which reduces the overall inner diameter to 1.75 mm. The air nozzle position relative to the cylinder could be adjusted automatically by using a computer controlled traverse system. The traversing speed could be varied from 1 mm/sec to 10 mm/sec along the tube. A constant temperature anemometer with single-sensor of normal probe was used to measure the acoustic velocity fluctuation along the tube at different modes and flow jet velocities. The traverse system was used to move the probe with an increment of 1 mm and 1 cm in the

radial and axial directions respectively in the tube. The scanning area is 8×12 cm above the nozzle (the radial and axial distance respectively). Figure (2) shows a schematic diagram of the air nozzle and hot-wires probe arrangement.

The transparent cylindrical tube has a length and inner diameter of 0.755 m and 0.125 m respectively. The chamber is made of transparent material with a wall thickness of 3 mm. The loudspeaker (BUMPER model) has a maximum power of 350 W and a frequency range from 20 Hz to 4000 Hz. Its effective diaphragm radius and area are 8.75 cm and 0.02405 m^2 respectively. Since the loudspeaker has a larger diameter than the tube, a cone tube (cowl) is used to connect the loudspeaker and the transparent tube. The rear side of the speaker diaphragm is enclosed by a box (21 (width) x 21 (length) x 16 (height) cm), which ensures the loudspeaker to be a monopole source. The signal generating system consists of a signal generator (type J2B 10 mW) and an amplifier with impedance of 10 Ω.

A micro-manometer (PVM100) was used to measure the static pressure along the tube at different modes. The PVM100 is designed to read positive or negative pressure up to 3500 Pa with pressure resolution of 1 Pa. A sound pressure meter was used to measure the sound pressure level ($P_{ref.} = 20\mu Pa$).National Instrument DAQ card and Labview 7 software have been applied for data acquisition, monitoring and analysis.

THEORETICAL CONSIDERATION

To provide some theoretical background, one dimensional plane wave acoustic equation has been solved by simplifying the experimental rig. From the experimental setup it can be seen that the acoustic confinement is not a simple cylindrical tube due to the existence of the cowl. For simplicity, the cowl and the cylindrical tube can be considered as a single cylinder for acoustic analysis. This is acceptable since the wavelength of interest is much longer than the diameters of the two sections and one-dimensional assumption should be a good approximation, which is a valid assumption when the acoustic frequencies considered are low with respect to the critical frequency or the cut-off frequency (f_c) of the tube, and hence waves are considered planar, and all modes are longitudinal. The exact value of f_c depends on the shape of the pipe cross section. The cut-off frequency f_c is of the order of $c/2d$ where d is the widest diameter of the tube and c is the speed of the sound, [6, 11, and 12].

For a cylindrical tube filled with air, open at top end and closed by a loudspeaker at the bottom end, the first mode frequency (f) corresponds (n = 1) to a node pressure at the open end, and anti-node pressure at the distance of $(2n-1)\lambda/4$ from the open end of the tube ($z = L'$). In the equation, n is an integer number, L' is the total length of the tube and the cone tube (cowl), and λ is a wavelength. The higher-order modes occur at n = 2, 3, 4, …, as shown in Figure (3). It should be pointed out that the pressure node is not exactly at the top end of the tube in a practical system. In an open end tube the first mode frequency is $c/4L' = 75Hz$. Assuming room temperature of $20^{\circ}C$, the frequency of the first four modes is 75, 225, 375, and 525 Hz respectively. In the case of combustion, the estimation of the mode is complicated by the temperature variation. Assuming 1D plane wave in the tube, it can be demonstrated that the acoustic particle velocity and pressure in the cylindrical tube could be expressed as

$$u(z,t) = \frac{u_o}{\cos(kL')}\left(\cos\left(k\left(L'-z\right)\right)\right)\left(\cos\omega t\right)\right) \quad (1)$$

$$p(z,t) = -\frac{\rho_o c u_o}{\cos(kL')}\left(\sin\left(k\left(L'-z\right)\right)\right)\left(\sin\omega t\right)\right) \quad (2)$$

Where,

ρ_o is the density of the air,

k is the wave number,

ω is the angular frequency,

u_o is the *rms* velocity of the loudspeaker diaphragm.

From Eqs. 1 and 2 it is clear that the mean acoustic particle velocity and pressure along the whole cylindrical tube should be zero. However the above equations have neglected the hydrodynamic and geometric near field effects, which may be important. Experiments are necessary for further physical insights. It can also be shown that the root mean square of the normalised velocity (u_{rms}) by $u_{rms}(L')$ and normalised acoustic pressure (p_{rms}) by $p_{rms}(0)$ could be expressed as:

$$\frac{u_{rms}(z)}{u_{rms}\left(L'\right)} = \left|\left(\cos\left(k\left(L'-z\right)\right)\right)\right| \quad (3)$$

$$\frac{p_{rms}\left(z\right)}{p_{rms}\left(0\right)} = \left|\left(\sin\left(k\left(L'-z\right)\right)\right)\right| \quad (4)$$

At resonance the anti-node pressure (node velocity) locations are given by $z = 2(m-1)L'/(2n-1)$ (by assuming $(L'-(2n-1)\lambda_n/4)$ is very small), so that p(z) is at a maximum. At the first mode (n = 1), the pressure anti-node (velocity node) location occurs only at m=1, (z = 0). At the second mode (n = 2), pressure anti-nodes (velocity nodes) locations occur at m =1 and 2 (z = 0, $2L'/3$). At the third mode (n = 3), pressure anti-nodes (velocity nodes) locations occur at m = 1, 2 and 3 (z = $0, 2L'/5, 4L'/5$).

Figure (4) depicts the variation of the normalised velocity $\left(u_{rms}(z)/u_{rms}(L')\right)$ variations as a function of the transparent tube length (L = L'- cowl length) for the first four modes, by using Eqs. (3). At z = 0, the *rms* velocity is u_o and at z =L', $\partial u/\partial z = 0$.

RESULTS AND DISCUSSIONS

To evaluate the relative amplitude of *rms* acoustic pressure at different excitation frequencies, the *rms* pressure at the pressure anti-node is measured. The *rms* pressure is measured by a microphone, which is located at just above the loudspeaker as shown in Figure (1), because this location always has maximum *rms* acoustic pressure amplitude. Where as, the other pressure anti-node locations vary with the excitation frequency. The excitation frequency applied varies from 20 Hz, which is the lowest frequency response of the loudspeaker to = 550 Hz with an increment of 1 Hz. The voltage applied to the loudspeaker is 16 volts. By using the data acquisition system, the digital signal generator is connected to the loudspeaker through a digital to analogue (D/A) channel and the signals picked up by the microphone which is connected to the data acquisition system through the analogue to digital (A/D) channel.

Figure (5) shows the power spectrum at the fundamental excitation frequency of 75 Hz. Sub-harmonics are clearly seen in the figure, which correspond to the higher order harmonics of the tube (225, 375, 525 Hz,…) with ratios of 1: 3: 5: …

Figure (6) illustrates the first four wave modes of the measured *rms* velocity and the *rms* pressure along the transparent tube. These were obtained by moving the probes along the tube whilst keeping the loudspeaker at a constant applied voltage. The trends of the curves are similar to the theoretical calculation of the open top cylindrical tube with an end-mounted loudspeaker. The results have shown that when the *Urms* is at a maximum the *Prms* is at a minimum and vice versa. And always the maximum velocity is at the open end of the tube. From Figure (6), it can also be seen that the pressure fluctuations (*rms*) are periodic along the tube and so are the velocity fluctuations.

Figure (7) shows the static pressure changes along the tube when the air-filled cylindrical tube is excited at 225 Hz. A micro-manometer was used to measure the static pressure. At the top end of the tube the pressure is observed to be equal to the ambient pressure. The figure shows that at the second mode (225 Hz) the static pressure drop increases until the middle of the tube (anti-node pressure) and also the maximum air flow rate has been observed at this location, which is referred to as the rarefaction regime.

Figure (8) shows the axial velocity at the centreline and 5 mm above the nozzle of the air jet with a constant air flow rate (150 ml/min) and with an increase in the air flow rate due to excitation at the second mode of excitation (f_e = 225 Hz) as a function of the voltage applied to the loudspeaker, the figure also shows the air flow rate as a function of voltage applied to the loudspeaker. It can be seen from the figure that the jet velocity is strongly affected by the acoustic excitation. As can be seen at zero volts, the axial velocity is less than 1 m/sec. The velocity has increased to about 7 m/sec at 14 volts and the air flow rate also increased from 150 ml/min without excitation to about 300 ml/min at 14 volts. When the applied voltage to the loudspeaker is low, the axial velocities are the same in amplitude for both of constant flowrate test case and unregulated flow case. But at a higher voltage there is a small discrepancy between the cases, which indicates that the volume flow rate change or difference has little effect on the jet velocity. This observation is interesting.

Note that the axial velocity has increased by seven times at 14 volts and the supply air flow rate change contributes little on this increase. The air around the jet is mixed with the air jet accelerated. This phenomenon has a good advantage for improving the combustion process. At this condition of excitation a laminar jet propane diffusion flame became completely blue in colour and shorter in height, and also the flame lifts off. This indicates that the acoustic excitation may have enhanced the mixing of the fuel gas and the surrounding air in this regime. The observation also reported by [7]. Figure (9) illustrates the jet diffusion flame without and with excitation (f_e = 225 Hz and at 3.8 volts applied to the loudspeaker). The fuel nozzle position is at the middle of the tube.

Figure (10) presents the contour map of the confined laminar air jet velocity with and without excitation. The left sub-figure shows the air jet without excitation. It can be clearly seen from the figure that the jet is narrow and symmetric to the jet centreline. The maximum mean velocity is observed at the centreline. The maximum velocity at 5 mm above the air nozzle exit is less than 1 m/sec. The right sub-figure shows the velocity map at an excitation frequency of 225 Hz and at an applied voltage of 5 volts. It

is clearly evident from the figure that the jet with excitation is more turbulent and the jet is not symmetric and the flow structure of the jet is completely different compared with the jet without excitation. Also, it is obvious that the excitation has a significant effect on the mean velocity. The maximum velocity is more than 3.5 m/sec at 5 mm above the air nozzle. Thus the velocity has increased more than three times compared to that of the air jet without excitation

Figure (11) shows the velocity profiles of the air jet with and without excitation at different positions above the jet nozzle (5, 25, 35 and 85 mm). it can be seen that the acoustic excitation has a strong effect on the velocity. From the sub-figures it is clear that the velocity with excitation is much higher than that of the jet without excitation. For example, at 5 mm above the nozzle, the maximum velocity of the jet without excitation at the centreline is about 0.85 m/sec, compared with the jet velocity of 3.75 m/sec with excitation. The same effect is observed for the other profiles at different positions. Also the figure shows that the velocity profiles of the air jet with excitation are wider than that of the jet without excitation.

Figures (10) and (11) seem to indicate that the acoustic excitation has a much strong effect on the jet part than the air surrounding the jet. In other words the excitation makes the high velocity region flow even further. The mechanism for causing this unusual behaviour is worth of further studies.

Figure (12) shows the power spectrum of the axial velocity at different positions along the air jet centreline, with and without excitation. It is clear from the figure that the peak frequency of the air jet has the same excitation frequency of the signal generator. The sub-harmonic ratio of the power spectrum is not the same as the acoustic sub-harmonics of a cylindrical tube. The jet velocity sub-harmonic ratio of the excited air jet is 1: 2: 3:…, while the acoustic sub-harmonics tube mode ratio is 1: 3: 5:…, as shown in Figure (5). Figure (12) shows also that the power spectrum of the excited air jet is at a strong harmonic mode. No sub-harmonics are observable without excitation. It can be seen that the peak frequency (424 Hz) is the same at different positions.

CONCLUSION

This paper has reported some important features of the flow characteristics of a laminar air jet in a loudspeaker induced standing wave. The article analysis has been carried out on standing wave and it was found that the experimental data agree with the theoretical results in general trends. Then the flow behaviour of laminar air jet in the standing was investigated. The results have shown that acoustic excitation has a strong effect on the flow characteristics of the jet and also on air suction rate, due to the negative static pressure induced in the cylindrical tube. The air suction rate is found to be sensitive to the excitation frequencies and the position along the cylindrical tube.

The acoustic and velocity characteristics of a laminar air jet under the second mode of excitation (225 Hz) have been measured experimentally in detail. The maximum effect of acoustic vacuum on air flow rate was observed when the pressure anti-node of the exciting frequency coincides with the pressure anti-node of the natural frequency of the cylindrical tube. The position of the air nozzle has a major influence on the air flow rate. A very important observation is that the velocity close to the air nozzle is much higher than expected when under acoustic excitation. It is observed that acoustic excitation could cause the high velocity region to flow even further.

The above observations demonstrate that an acoustic wave, especially a standing wave, interacts with flow field in a very complex way. Further investigation is of great importance to the fundamental understanding of the properties of an acoustic wave.

REFERENCES

[1] Halliday D. and Resnick R. (1978) "Physics" Third Edition.

[2] Hathout, J. P., Annaswamy, A. M., Fleifil, M. and Ghoniem,.A. F. (1998). "Model-based Active Control Design for Thermoacoustic Instability," *Combustion Science and Technology,* 132: 99–138.

[3] McManus, K. R., Poinsot, T. and Candel, S. M., (1993). "A review of Active Control of Combustion Instabilities," *Progress in Energy and Combustion Science,* 19: 1-29.

[4] Heckl, M. A. (1988). "Active Control of the Noise from a Rijk tube," *Journal of Sound and Vibration,* 124(1): 117-133.

[5] Lang, W., Poinsot, T. and Candel, S. (1987). "Active Control of Combustion Instability," *Combustion and Flame,* 70: 281-289.

[6] Hathout, J. P. (1999). "Thermoacoustic Instability," *Reacting Gas Dynamics Computational Lab, Cambridge.* (*http://centaur.mit.edu/rgd/lecomb.pdf)*

[7] Saito, M., Sato, M. and Nishimura, A. (1998). "Soot suppression by acoustic oscillated combustion," *Fuel,* Vol. 77 No. 9/10: 973-978.

[8] Mozurkewich, G. (2002). "Heat transport by acoustic streaming within a cylindrical resonator" *Applied acoustics*, 63: 713-735.

[9] Ng, W. B., Salem, A. F. and Zhang, Y. (2003) "Three-dimensional visualization of diffusion flame shapes under acoustic excitation using stereoscopic imaging and reconstruction," *Journal of visualization*, 6(4): 329-336.

[10] Farhat, S. A., Ng, W. B. and Zhang, Y. (2005) "Chemiluminescent Emission Measurement of a Diffusion Flame Jet in a Loudspeaker Induced Standing Wave," *Journal of fuel.*

[11] Temkin, S., (1981). "Elements of Acoustics." *Canada*, 164-165.

[12] Rienstra, S. W. and Hirschberg A., (2003) "An Introduction to Acoustics," *Eindhoven University of Technology*, pp. 70-71.

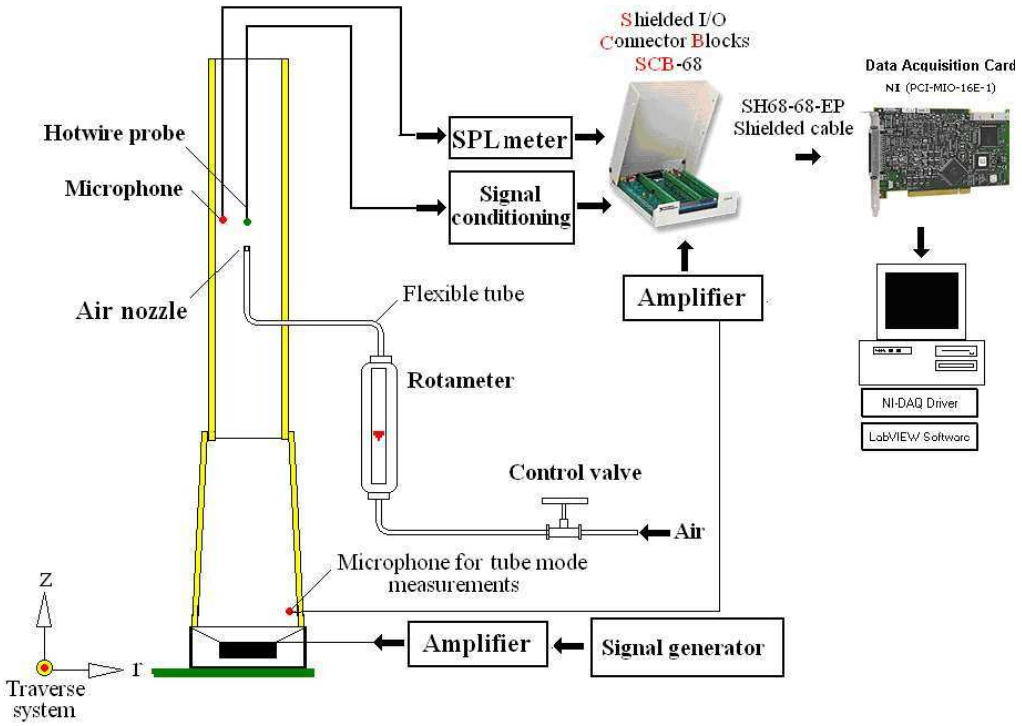

Figure 1: Experimental setup.

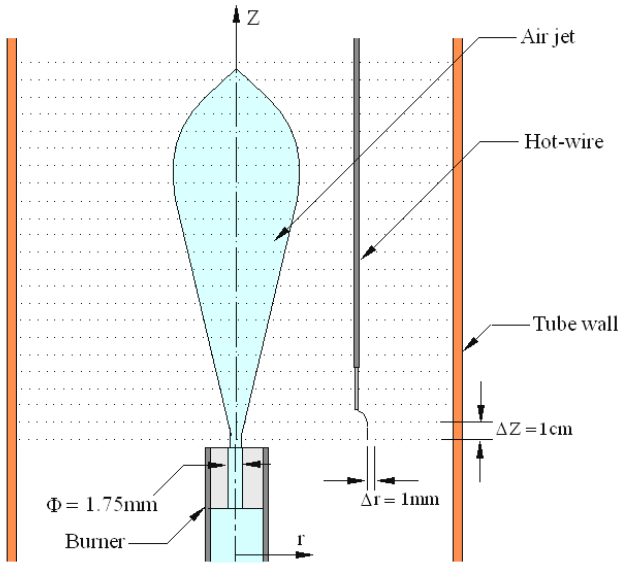

Figure 2: Schematic diagram of air nozzle and hot-wire probe arrangement.

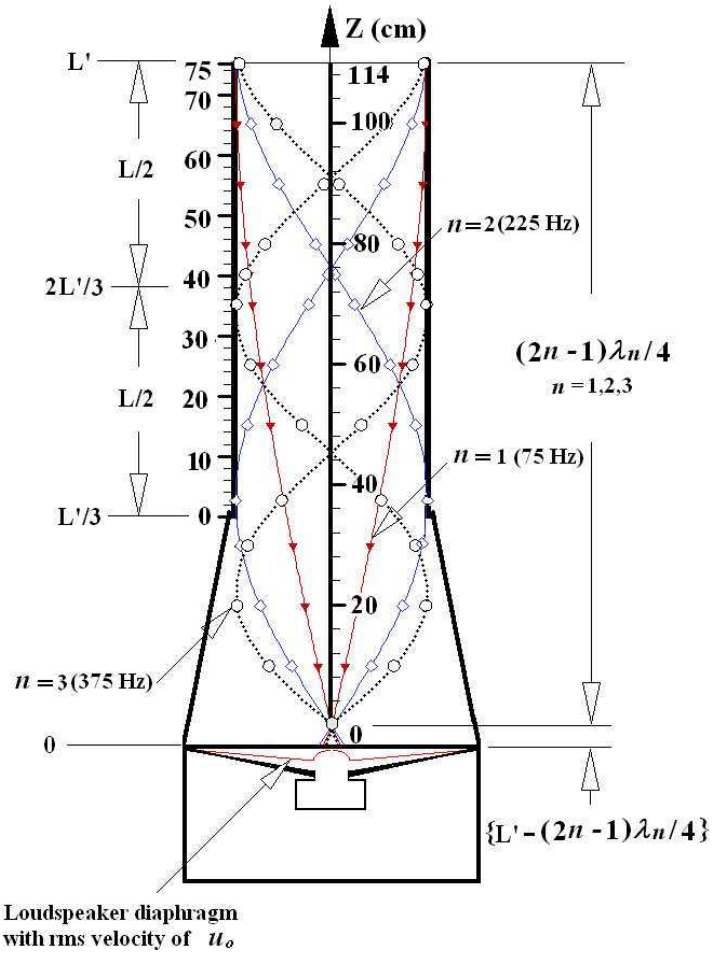

Figure 3: Illustrations of the various acoustic modes and dimensions (L' is the total tube length, L is the tube length without the cowl and λ is the wavelength).

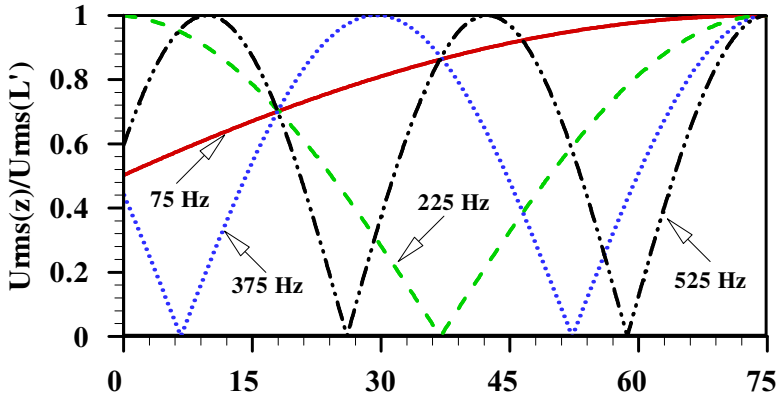

Figure 4: First four theoretical velocity and acoustic pressure modes along the tube without the cowl.

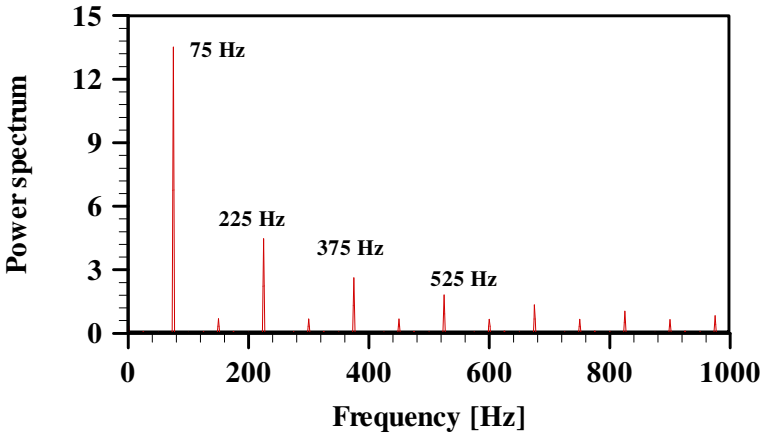

Figure 5: Power spectrum of the fundamental mode (75 Hz) of the tube.

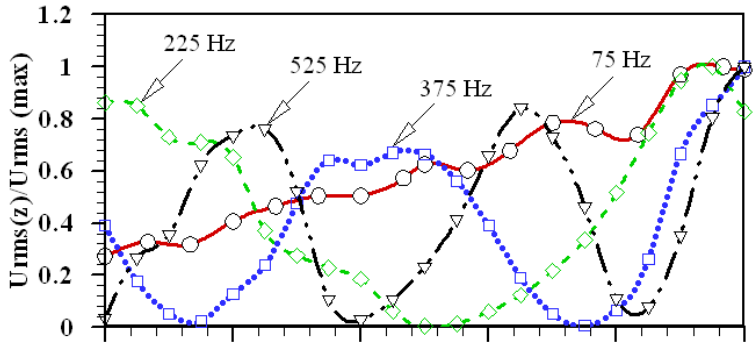

a – First four experimental velocity modes.

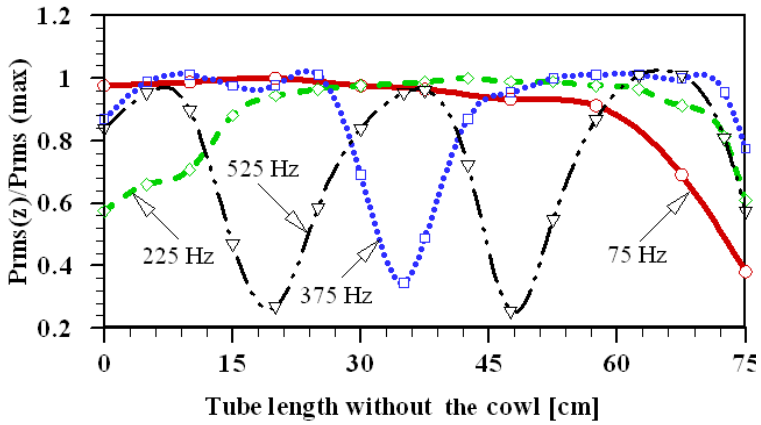

b – First four experimental acoustic pressure modes.

Figure 6: First four experimental longitudinal velocity and acoustic pressure modes of the tube without the cowl.

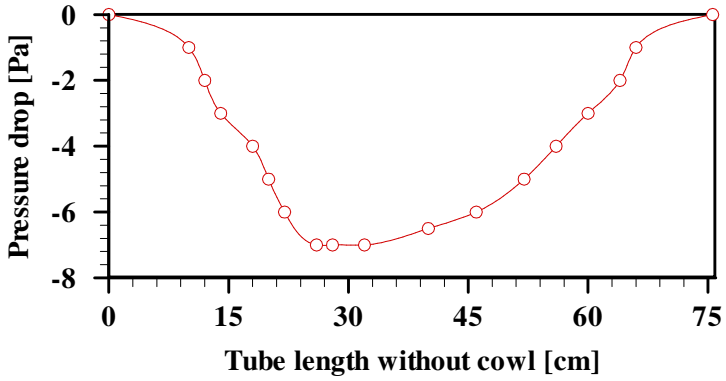

Figure 7: Static pressure along the tube axis, at n = 2 (225 Hz).

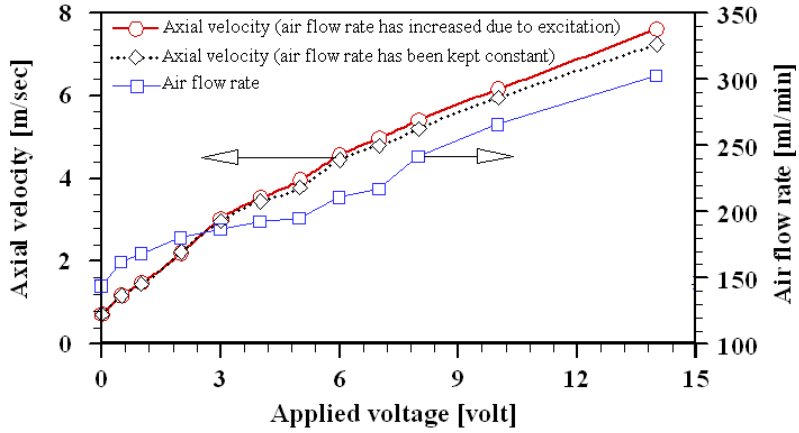

Figure 8: Axial velocity with constant air flow rate (150 ml/min) and with increase of air flow rate due to excitation and air flow rate as a function of applied voltage z = 37.5 cm.

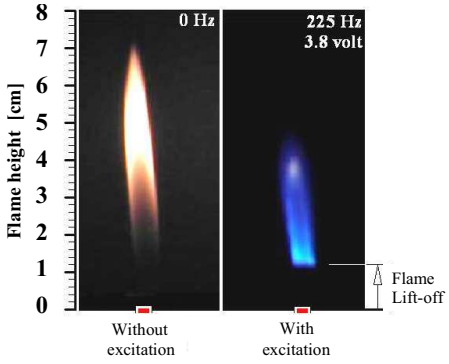

Figure 9: Laminar jet diffusion flame without and with excitation (f_e = 225 Hz and 3.8 Volts), burner position at the middle of the tube.

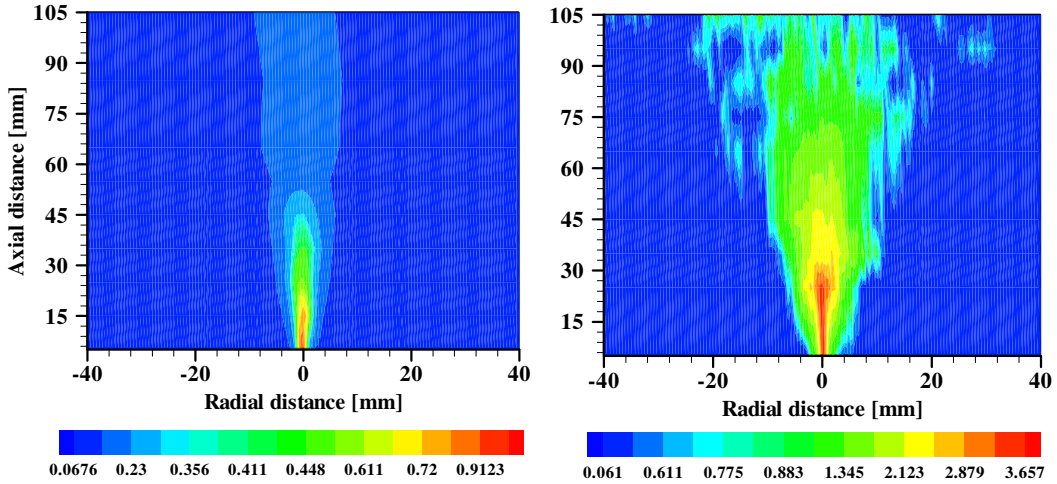

Figure 10: Flow structure of the Air jet at the middle of the tube (37.5 cm from the bottom of the tube) with and without excitation (f_e = 225 Hz, voltage applied to the loudspeaker is 5 volt; initial air flow rate is 180 ml/min).

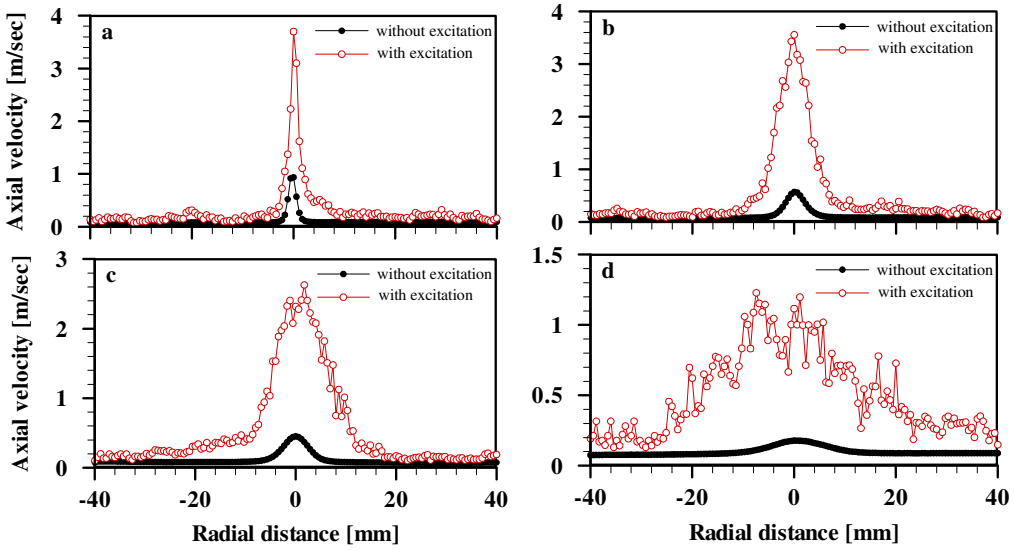

Figure 11: Velocity profile of the air jet with and without excitation at different position above the nozzle (a) – at 5 mm, (b) – at 25 mm, (c) – at 35 mm and (d) – at 85 mm. The excitation frequency is 225 Hz.

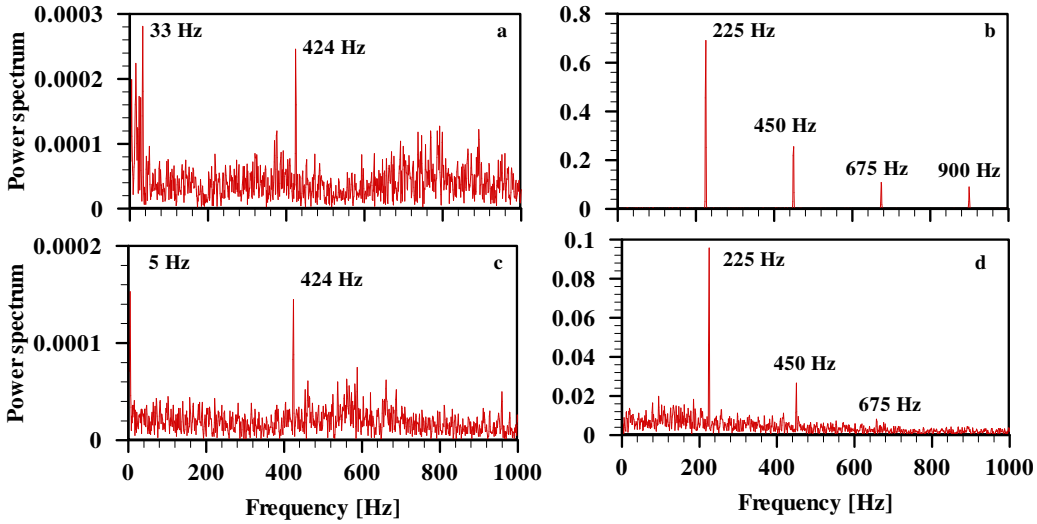

Figure 11: Power spectrum of the axial velocity at different position along the centreline of the air jet with and without excitation, a – without excitation, at 5 mm above the nozzle, b – with excitation (f_e = 225 Hz), at 5 mm above the nozzle), c - without excitation, at 25 mm above the nozzle, d – with excitation (f_e = 225 Hz), at 25 mm above the nozzle (the voltage applied is 5 volts and the air flow rate is 180 ml/min).